Simulating Laminar Flow over a Flat Plate with an Isothermal Wall in SU2

Kedar R. Naik

Stanford University

knaik@stanford.edu

February 5, 2015

Abstract

Several simulations of flat-plate flow were performed using SU2 at NASA Glenn from June to July of 2014. Here, one specific case has been investigated again, namely: laminar flow over a flat plate with an isothermal wall boundary condition. The temperature difference between the freestream and the surface is relatively small when compared to that of the previous simulation. Moreover, a low freestream Mach number has been chosen in an attempt to minimize the effects of compressibility. Various quantities of interest from this new simulation have been plotted. Where appropriate, computational results have been compared with analytical solutions. The purpose of this report is to assist work on thermal boundary layers that is currently ongoing at NASA Glenn.

Preliminaries

The physical flow parameters of this simulation, as well as the numerical methods used, are described below.

Flow Conditions

This case simulates the laminar flow of air ($\gamma = 1.4$) over a flat plate held at a constant temperature, T_w. Specific conditions of the flow are listed below.

$$
\begin{array}{ll}
c_p = 1005\,\text{J}/(\text{kg K}) & \text{specific heat capacity} \\
k = 0.026\,18\,\text{W}/(\text{m K}) & \text{thermal conductivity} \\
p_{t_{in}} = 100\,000\,\text{Pa} & \text{inlet stagnation pressure} \\
p_{out} = 99\,303.1\,\text{Pa} & \text{outlet static pressure} \\
Pr = 0.72 & \text{Prandtl number} \\
T_{t_{in}} = 300\,\text{K} & \text{inlet stagnation temperature} \\
T_w = 350\,\text{K} & \text{isothermal wall temperature} \\
T_\infty = 300\,\text{K} & \text{freestream temperature} \\
U_\infty = 34.7715\,\text{m/s} & \text{freestream velocity} \\
\mu = 1.844\,92 \times 10^{-5}\,\text{N s/m}^2 & \text{dynamic viscosity} \\
\rho_\infty = 1.137\,53\,\text{kg/m}^3 & \text{freestream density}
\end{array}
$$

N.B. The static pressure at the outlet, p_{out}, was computed using the isentropic relation, viz.

$$
p_{out} = p_{t_{in}} \left[1 + \frac{1}{2}\left(\gamma - 1\right) M_\infty^2 \right]^{-\frac{\gamma}{(\gamma - 1)}}.
$$

A low freestream Mach number of $M_\infty = 0.1$ was selected to minimize the effects of compressibility.

Numerical Methods

The Navier-Stokes equations without a turbulence model were used to model laminar flow. The specific algorithms and relaxation schemes used to solve the problem are listed below.

CFL number on finest grid: 3.0

linear solver: FGMRES

linear solver preconditioner: LU-SGS

multigridding levels: 1

convective scheme: Roe, 2nd-order

Results

Some salient results from the simulation done in SU2 are presented here. This includes evidence of numerical convergence as well as extracted profiles of skin friction, temperature, heat transfer, and density.

Numerical Convergence

The problem was considered to be converged after seeing the residual in density fall five orders of magnitude. A plot of the residual history is found in Fig. 1.

Skin Friction

Fig. 2 compares the coefficient of skin friction, C_f, calculated by SU2 with that of the analytical solution by Blasius:

$$C_f(x) = \frac{0.6641}{\sqrt{Re_x}},$$

where $Re_x = \frac{U_\infty x}{\nu}$ is the local Reynolds number. Checking the skin friction coefficient is generally a good way of assessing the quality of a laminar, flat-plate simulation.
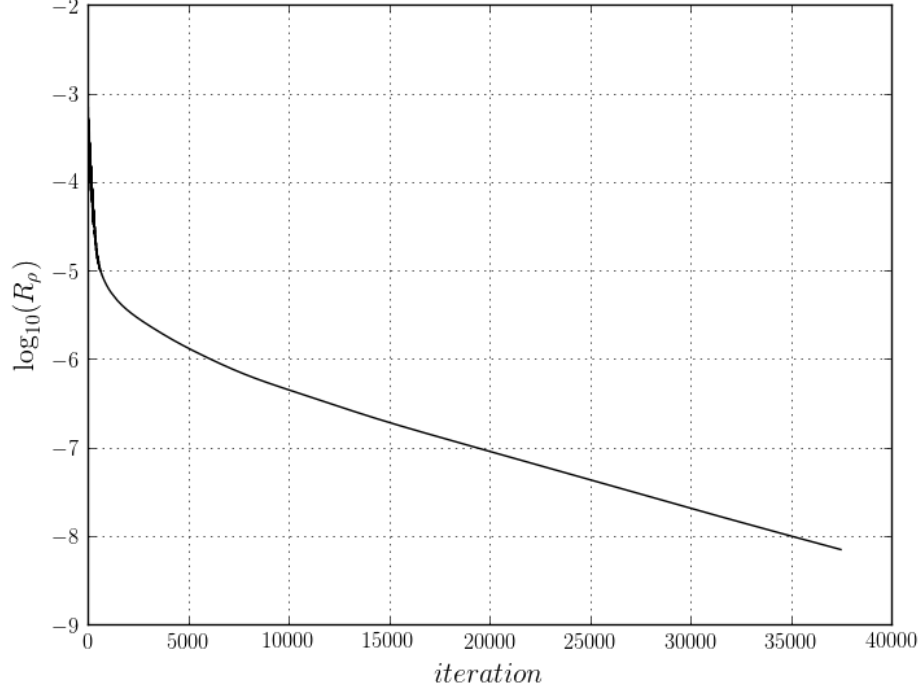
Figure 1: The convergence history of the density residual, R_ρ.

Thermal Boundary Layer

The isothermal wall condition allows one to investigate the development and growth of a thermal boundary layer along the surface of the plate. In Fig. 3, nondimensionalized temperature,

$$\theta = \frac{T - T_w}{T_\infty - T_w},$$

has been plotted against nondimensionalized wall distance,

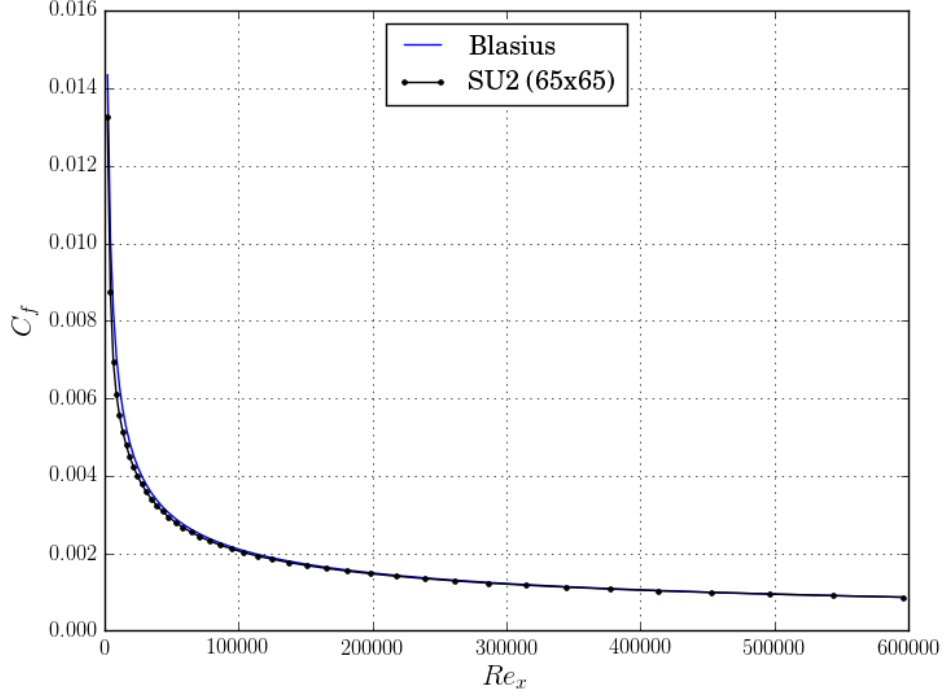$$\eta = \frac{y}{\sqrt{\frac{\nu x}{U_\infty}}},$$

Figure 2: Variation in C_f along the length of the plate plotted as a function of local Re.

where $\nu = \mu/\rho$ denotes the kinematic viscosity. In Fig. 3, the cross-section has been taken along the outlet boundary — i.e. at the end of the plate.

The temperature profile extracted from the SU2 output is compared against the analytical solution of Pohlhausen as well as the Crocco-Busemann relation, which is designed to account for the effects of compressibility. Pohlhausen's solution is given by

$$
\theta_{Pohlhasusen} = 1 - \frac{\int_{\eta}^{\infty} \left(\frac{d^2 f}{d\eta^2}\right)^{Pr} d\eta}{\int_{0}^{\infty} \left(\frac{d^2 f}{d\eta^2}\right)^{Pr} d\eta},
$$

where f is the well-known solution to the Blasius equation. The Crocco-Busemann relation is given in terms of temperature at a given point in the domain, namely:

$$T_{CB} = T_w + (T_{aw} - T_w)\frac{u}{U_\infty} - \frac{ru^2}{2c_p}.$$

Here, u is the local velocity in the x direction, r is the so-called "recovery factor" given by $r = \sqrt{Pr}$, and T_{aw} denotes the *adiabatic wall temperature*, defined as

$$T_{aw} = T_\infty + \frac{rU_\infty^2}{2c_p}.$$

In Fig. 3, the temperature given by the Crocco-Busemann model, T_{CB}, has been nondimensionalized as follows:

$$\theta_{CB} = \frac{T_{CB} - T_w}{T_\infty - T_w},$$

Nusselt Number

The rate of heat transfer along the surface of the plate, q_w, was calculated by SU2 and used to compute a distribution of local Nusselt number,

$$Nu_x = -\frac{q_w x}{k(T_w - T_\infty)}.$$

Fig. 4 compares the result from simulation with the analytical solution of Blasius, viz.

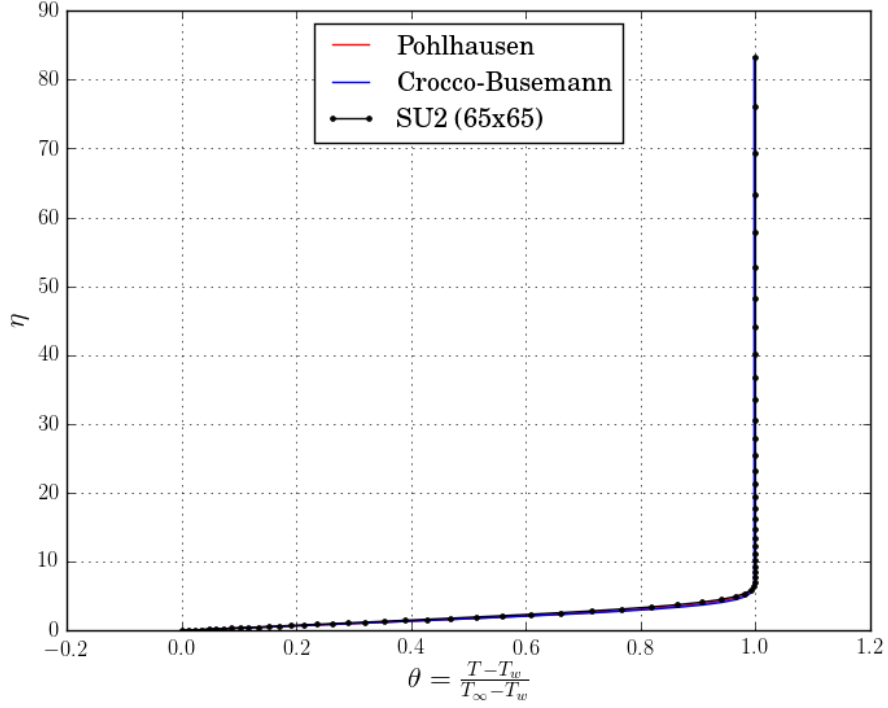$$Nu_{x_{Blasius}} = 0.332\sqrt{Re_x}Pr^{1/3}.$$

Figure 3: Nondimensionalized temperature profiles at the outlet.

Density Variations

Naturally, when using a compressible solver, changes in temperature will lead to changes in density. Lest comparisons to the incompressible Blasius solutions be suspect, Fig. 5 shows how the flow density varies through the boundary layer at the trailing edge of the plate. Whether or not this change in density is too large for a comparison to be made between this simulation and the Blasius solutions is a matter of the analyst's discretion.

Summary

Some of the salient results from an isothemeral, laminar, flat-plate simulation have been presented. When deemed appropriate, CFD results from SU2 have
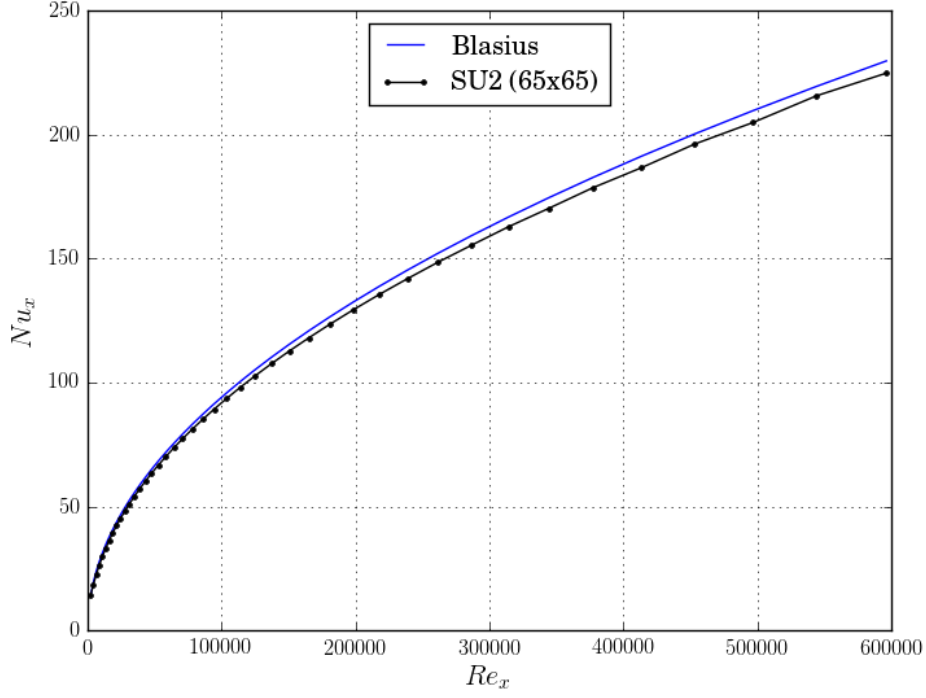
7

Figure 4: Local Nusselt number plotted along the length of the plate.

been compared again the analytical solutions of Blasius, Pohlhausen, and Crocco-Busemann. On balance, it appears that prescribing a small temperature difference, $T_w - T_\infty$, as well as a low inlet Mach number allows the output from a compressible solver to be reasonably compared with incompressible analytical results. This appears to be the case for both aerodynamics as well as heat transfer.
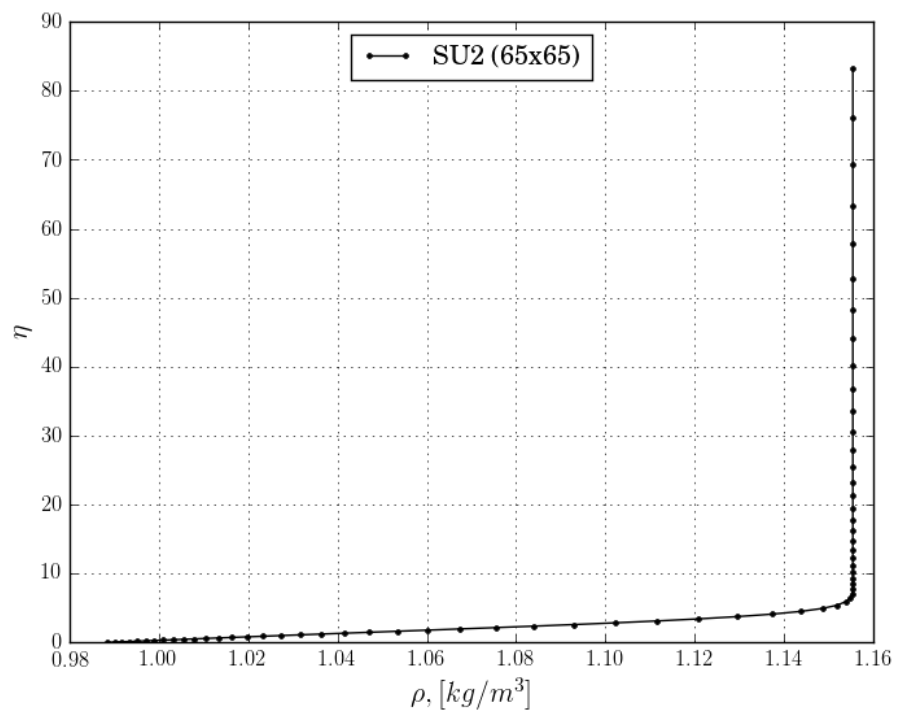
Figure 5: Density profile observed at the mesh outlet.